# Deposition Fraction of Aerosol Particles in a Human Oral Airway Model on Stable Condition

**Lianzhong Zhang[1,2] *, Hongjuan Cheng[1], Chenbing Zhang[1], Zhaojin Xu[1], Jian Ye[1]**

[1] *Institute of Physics, Nankai University, Tianjin 300071*
[2] *Institute of Environmental Science and Engineering, Nankai University, Tianjin 300071*

## Abstract

In this paper, the fluid field of a human oral airway model is gained though the simulation method. After computing the system in the stable condition, the deposition efficiencies of aerosols in different Stokes number are obtained and the trace of typical aerosols are figured.

***Keywords*:** Aerosol; Oral airway model; Deposition fraction.

## INTRODUCTION

The dynamic investigation of aerosol in the human respiratory system is an interdisciplinary field of respiration hydrodynamics and aerosol dynamics (Wen, 1996; Edwards *et al.*, 1997). The study of aerosol behaviour in the human respiratory system is important to the treatment of many diseases for several reasons. First of all, masses of micro-particles or venomous gases in the inhaled aerosol can cause disorders in the lungs or other organs in the body (Pleil *et al*., 2000; Wichmann and Peters, 2000). Secondly, the study of aerosol deposition mechanism is a new method in medical treatment; for example, in clinic therapy, insulin in the aerosol state is more easily absorbed by the body than liquid insulin (John *et al*., 1999).

In this paper, we mainly discuss the dynamic action of aerosol in the oral airway. Because of the geometric complexity of the oral airway, a transition is possible from a laminar to a turbulent flow. The result would be far from the fact if we used the $k-\varepsilon$ turbulent model during the simulation process, because that model is fit for the high-Reynolds-number condition, but not the low-Reynolds-number condition (Stapleton *et al*., 2000). Based on the anthropotomy model method, we constructed a relatively simple, but representative, geometry model with the help of computer software. This model contains the oral cavity, pharynx, larynx, and trachea. The model mesh was segmented and tessellated. In this simulation, an air-particle two-phase flow was imported and operated under a steady-state condition. The flow field, particle deposition efficiencies, and trajectories were investigated to depict the results.

* Corresponding author. Tel.: 86-22-23503454, Fax: 86-22-23503454
E-*mail address*: zhanglz@eyou.com

# TRANSPORT EQUATIONS AND ORAL AIRWAY MODEL

### *Transport equations*

This model was developed to simulate the incompressible fluid in the air-particle two-phase flow, continuous medium in the air flow, non-interacting spherical micron-particle transport, and deposition in the oral airway. The expiratory flow was not calculated in the simulation, since expiratory oral deposition deficiency is much less important than the inspiratory. Because of the medium disturbance accrued by particle movement in the flow field, there was a transition of laminar-to-turbulent air flow, which entered the lung airway as a laminar flow. Zhang et al. (2002) validated that simulation results based on the low-Reynolds-number (LRN), $\kappa$-$\omega$, model agrees better with experiment data, so we selected and adapted Wilcox's (1998) LRN $\kappa$-$\omega$ model for internal flow.

Thus the fluid-particle transport equation can be written as:

***Continuity***:

$$\vec{\nabla} \cdot \vec{u} = 0 \tag{1}$$

***Momentum***:

$$\frac{\partial \vec{u}}{\partial t} + \left(\vec{u} \cdot \vec{\nabla}\right)\vec{u} = -\frac{1}{\rho}\vec{\nabla} p + \nu \nabla^2 \vec{u} \tag{2}$$

where $\vec{u}$ is the velocity vector, $p$ is the pressure, $\nu = \mu/\rho$ is the fluid kinetic viscosity, $\rho$ is the fluid density, and $\mu$ is the fluid dynamic viscosity.

According to Newton's second law:

$$m_p \frac{d\vec{u}_p}{dt} = \sum \vec{F}_p \tag{3}$$

After being simplified by Cheng *et al.* (1999), the Stokes number can be expressed as:

$$St = \frac{\rho_p d_p^2 U}{9\mu D_1} \tag{4}$$

where $m_p$ is the mass of a single-spherical particle, $\vec{u}_p$ is the particle velocity vector, $U$ is the mean inlet velocity, $D_1$ is the minimum hydraulic diameter, $d_p$ is the particle diameter, $\rho_p$ is the particle density and $\sum \vec{F}_p$ are the forces acting on it.

### *$\kappa$-$\omega$ turbulent equation*

At the inlet, the initial values for $\kappa$ and $\omega$ were assigned from the following empirical relation:

$$k = 1.5(I \times u_{mean})^2 \quad \text{and} \, \omega = \frac{\sqrt{k}}{0.3D} \tag{5}$$

where $\kappa$ is the turbulent kinetic energy, $\omega$ is the dissipation per unit turbulence kinetic energy, $I$ is the turbulence intensity which usually is 0.037, $u_{mean}$ is the mean axial velocity at the inlet and $D$ is the diameter of the inlet tube.

***Particle trajectory equation***:

$$\frac{d}{dt}(m_P u_i^P) = \frac{1}{8}\pi\rho d^2 C_{DP}(u_i - u_i^P)\left|u_i - u_i^P\right| \tag{6}$$

where $u_i^P$ and $m_P$ are the velocity and mass of the particle, respectively, and $C_{DP}$ is the drag-force coefficient given by:

$$C_{DP} = C_D / C_{slip} \tag{7a}$$

where

$$C_{DP} = \begin{cases} 24/\mathrm{Re}_P & for \quad 0.0 < \mathrm{Re}_P \le 1.0 \\ 24/\mathrm{Re}_P^{0.646} & for \quad 1.0 < \mathrm{Re}_P \le 400 \end{cases} \tag{7b}$$

And the particle Reynolds number is:

$$\mathrm{Re}_P = \rho\left|u_i - u_i^P\right| d / \mu \tag{7c}$$

$C_{slip}$ in Eq. (2-7a) can be found in Clift *et al.* (1978). Here $u_i$ is the instantaneous fluid velocity which $u_i = \bar{u}_i - u_i'$ , where $\bar{u}_i$ is the time-averaged or bulk velocity of the fluid, and $u_i'$ is its fluctuating component. According to Gosman and Ioannides (1981), it can be expressed as:

$$u_i' = \lambda(\frac{2}{3}k_i)^{1/2} \tag{8}$$

Thus, the randomicity of turbulence is modeled as the product of time-averaged turbulence energy and a random number $\lambda$ with zero-mean, variance of one and Gaussian distribution.

***Oral airway model***

Based on data (i.e., the cross-sectional area and the perimeter of the entire oral cavity, pharynx, and larynx area) reported by Cheng *et al.* (1999), we calculate the hydraulic diameter (4 × area / perimeter) and construct the oral airway model as depicted in Fig. 1.

**Fig. 1.** The oral airway model.

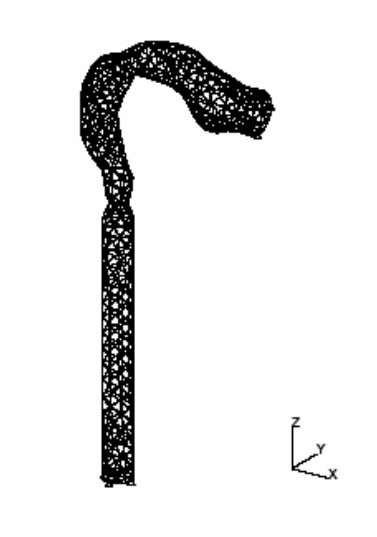

**Fig. 2.** Computational mesh.

## MODEL VALIDATION

For accurate computational fluid-particle dynamics (CFPD) simulations in the oral airway model, it is necessary to compare the simulation results with the experimental data. Cheng *et al*. (1999) provide a good experimental result for particle deposition fractions under three inhalation rates. Based on this, we did the computational simulations in which the grid consisted of about 70,000 cells and a global edge length of 0.1956 mm. Fig. 2 shows measured and CFPD-predicted deposition efficiencies for three inhalation rates.

As illustrated in Fig. 3, the simulation results agree with the experimental data, so the present computer geometry model is valid enough.

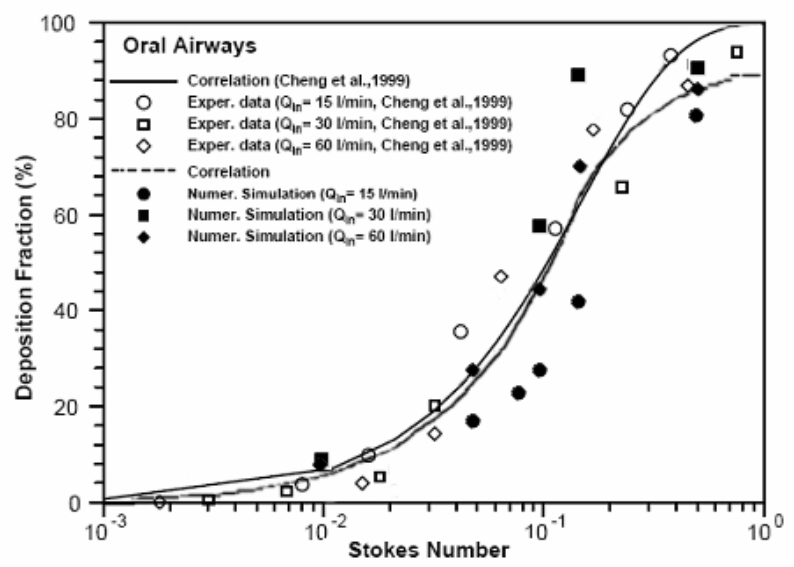


**Fig. 3.** Comparison of simulated and experimental particle-deposition fractions in the oral airway model under three inhalation rates.

## RESULTS AND DISCUSSION

### *Velocity fields*

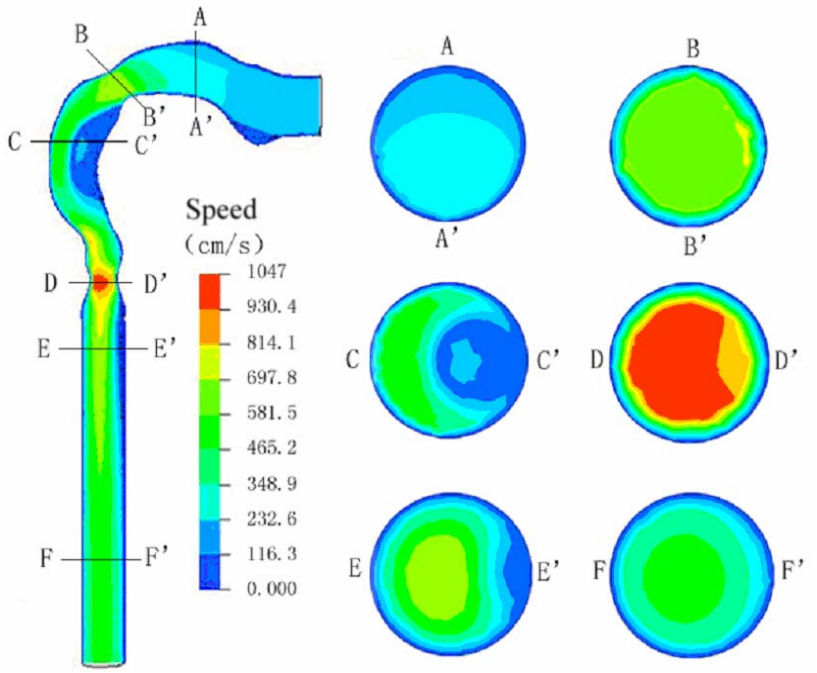


**Fig. 4.** Velocity profiles in the oral airway for $Q_{in} = 30l/\min$. The left panel exhibits mid-plane (Y = 0 plane) velocity contours. The right panels are the different cross-sectional views.

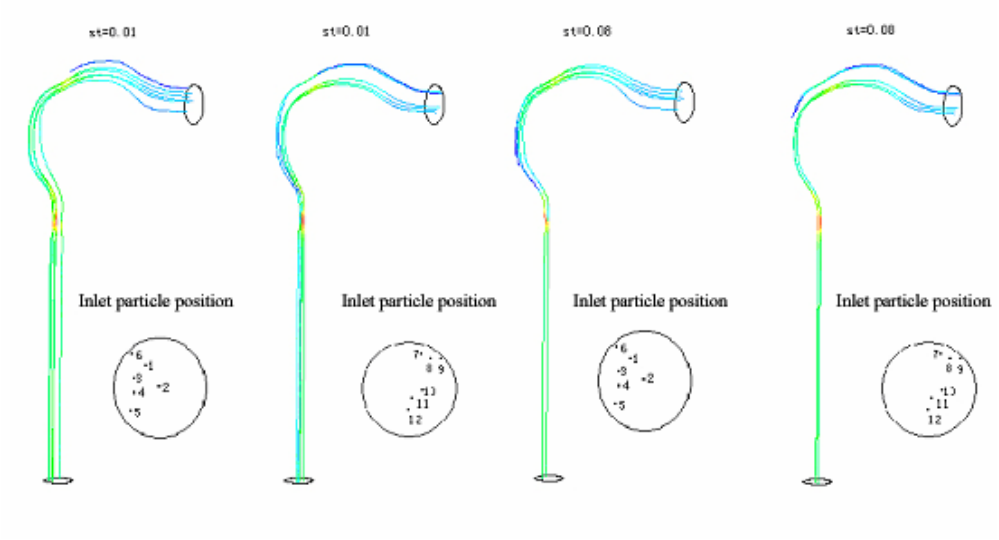


**Fig. 5.** Selected particle release positions and airway trajectories at $Q_{in} = 15l/\min$.

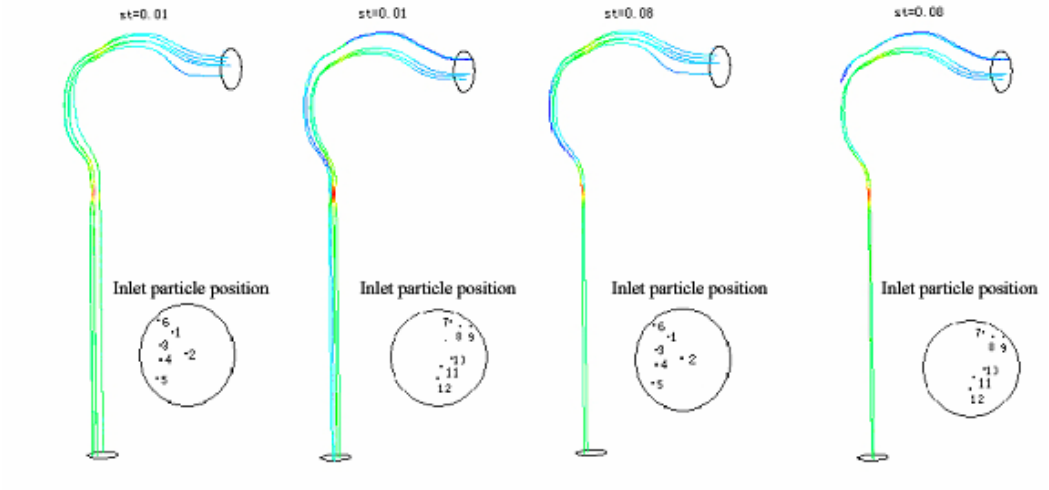


**Fig. 6.** Selected particle release positions and airway trajectories at $Q_{in} = 30l/\min$.

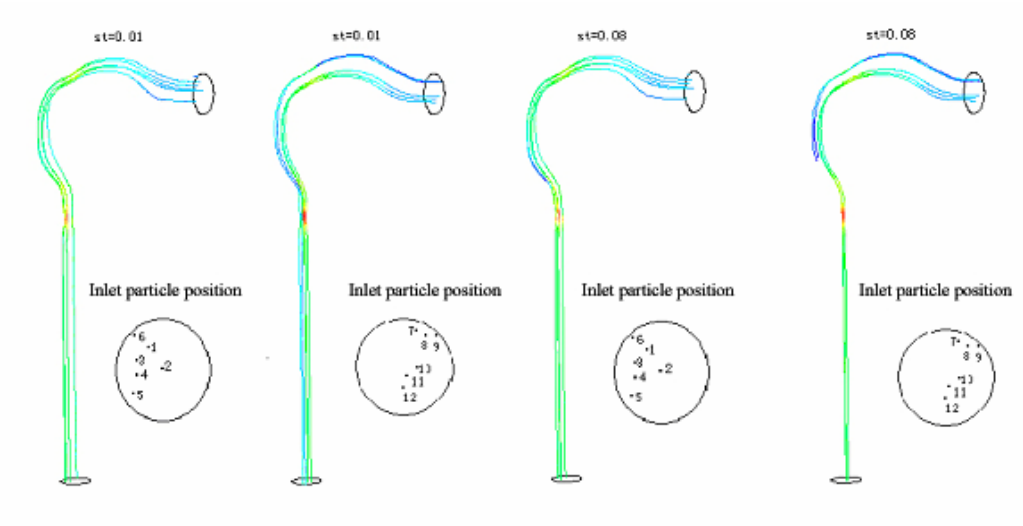


**Fig. 7.** Selected particle release positions and airway trajectories at $Q_{in} = 60\ l/\min$.

### *Particle trajectories*

In this simulation, we selected 12 particles randomly at the oral-airway inlet point and studied the effects of different Stokes numbers on their trajectories and deposition fraction under different flow rates. We chose different particle diameters, densities, and Reynolds numbers to obtain the condition with different Stokes numbers. Results indicate that particle deposition efficiencies increased with Stokes number increases. We also found that smaller particles deposit more easily under turbulent flow, further proving the theory established by Schlesinger and Lippman (1976).

### *Particle deposition fractions*

**Table 1.** The effect of Stokes number in different inhalation models on deposition fraction.

| $Q_{in}$=15 L/min | | $Q_{in}$=30 L/min | | $Q_{in}$=60 L/min | |
|---|---|---|---|---|---|
| Stokes number | Deposition fraction | Stokes number | Deposition fraction | Stokes number | Deposition fraction |
| 1E-3 | 0.01 | 1E-3 | 0.01 | 1E-3 | 0.01 |
| 0.01 | 9.25 | 0.01 | 9.46 | 0.01 | 9.18 |
| 0.05 | 30.89 | 0.05 | 30.83 | 0.05 | 18.82 |
| 0.08 | 49.51 | 0.08 | 49.84 | 0.08 | 25.36 |
| 0.1 | 64.18 | 0.1 | 49.38 | 0.1 | 30.83 |
| 0.15 | 98.55 | 0.15 | 77.56 | 0.15 | 46.23 |
| 0.5 | 100 | 0.5 | 95 | 0.5 | 89 |
| 0.95 | 100 | 0.95 | 100 | 0.95 | 100 |

Table 1 shows the effects of deposition fraction given by Stokes number at different inhalation-rate flow fields when Re = 2,000. It is not difficult to reach the conclusion that the particle DEs will increase as the Stokes number increases. Based on the calculation, we found that the increased particle consistency obviously can't affect the deposition fraction under a steady-state condition. While the Reynolds number is also an important factor affecting particle deposition fractions, the interrelationships are not known clearly enough; because, in different background flow fields, particle characteristics (density, diameter and so on) vary with the same Stokes number.

## CONCLUSIONS

A dynamic simulation of aerosol under the steady-state condition in the oral airway was developed to represent flow distribution, aerosol particle trajectories, and deposition fraction with different Stokes numbers. The following was concluded. The simulation of air-particle two-phase flow shows a comparatively simple and representational oral airway geometry model that provides a perfect equivalence platform for researching particle translation and deposition in oral airway.

Particle deposition is affected by both the Reynolds number and the Stokes number, but increased with Stokes number. Turbulence occurred after oral airway constriction, and high-level breathing could enhance the particle deposition in the trachea near the larynx. However, the fate of single particles was influenced by the trachea's position at the inlet, physical characteristics, and background flow field. Although more-complicated geometric features of the oral airway may be measurable for particle deposition, the simplicity of the presented simulations for exhibiting the main features of laminar-transitional-turbulent particle suspension flows in actual human oral airways could improve future investigations on the aerosol dynamic in the oral airway.

## ACKNOWLEDGMENTS

This research was supported by the National Natural Science Foundation of China (project number 10202007).

## REFERENCES

Cheng, Y. S., Zhou, Y., and Chen, B. T. (1999). Particle Deposition in a Cast of Human Oral Airways. *Aerosol Sci. Tech.* 31: 286-300.

Clift, R., Grace, J. R., and Weber, M. E. (1978). *Bubbles, Drops, and Particles*. New York: Academic Press.

Edwards, D. E., Justin, H., and Giovanni, C. (1997). Large Porous Particles for Pulmonary Drug Delivery. *Science* 276 (5320): 1868-1872.

Gosman, A. D. and Ioannides, E. (1981). Aspects of Computer Simulation of Liquid-Fueled Combustors. *Journal of Energy* 7: 482-490.

John, S. P., Julie, B., and Sudha, N. (1999). Inhaled Insulin. *Adv. Drug Deliv. Rev.* 35: 235-247.

Kim, C. S., Hu, S. C., Dewitt, P., and Gerrity, T. R. (1996). Assessment of Regional Deposition of Inhaled Particles in Human Lungs by Serial Bolus Delivery Method. *J. Appl. Physiol.* 81: 2203-2213.

Pleil, J. D., Smith, L. B., and Zelnick, S. D. (2000). Personal Exposure to JP-8 Jet Fuel Vapors and Exhaust at Air Force Bases. *Environ. Health Perspect.* 108: 183-192.

Schlesinger, R. B. and Lippman, M. (1976). Particle Deposition in the Trachea: In Vivo and in Hollow Casts. *Thorax* 31: 678-684.

Stapleton, K. W., Guentsch, E., Hoskinson, M. K., and Finlay, W. H. (2000). On the Suitability of $k-\varepsilon$ turbulence Modelling for Aerosol Deposition in the Mouth and Throat: A Comparison with Experiment. *J. Aerosol Sci*. 31(6): 739-749.

Wen, C. S. (1996). The Fundamentals of Aerosol Dynamics. *Singapore: World Scientific Publishing Company*: 105-148.

Wichmann, H. E. and Peters, A. (2000). Epidemiological Evidence of the Effects of Ultrafine Particle Exposure, Phil. *Trans. R. Soc. Lond. A.* 358: 2751-2769.

Wilcox, D.C. (1998). *Turbulence Modelling for CFD 2nd ed*. La Canada, CA; DCW Industries, Inc.

Zhang, Z., Kleinstreuer, C., and Kim, C. S. (2002). Micro-Particle Transport and Deposition in a Human Oral airway Model. *J. Aerosol Sci.* 33: 1635-1652 .

*Received for review, January 13, 2006*
*Accepted, May 23, 2006*